

# Single Axial Mode Operation of a Q-Switched Nd:YAG Oscillator by Injection Seeding

Y. K. PARK, G. GIULIANI, AND ROBERT L. BYER, SENIOR MEMBER, IEEE

**Abstract**—We have achieved stable Fourier transform limited single axial mode operation of an unstable resonator Nd:YAG oscillator by injection seeding of an external signal. A detailed theoretical and experimental treatment of axial mode selection via injection seeding is presented. Our study shows that the axial mode selection process in Q-switched lasers via injection seeding is quite different from the frequency locking in CW lasers via injection locking.

## I. INTRODUCTION

THE Q-switched high peak power Nd:YAG laser operating in a single axial mode is a very useful source for nonlinear and spectroscopic studies. Previously we have reported achieving stable single axial mode operation of an unstable resonator Nd:YAG oscillator by injecting an external signal [1]. This paper presents a theoretical and experimental discussion of axial mode selection via injection seeding of an external signal into the Q-switched Nd:YAG laser oscillator.

Interferometric methods of axial mode selection such as the use of a tilted etalon have provided stable single axial mode operation of CW Nd:YAG oscillators [2]–[4]. However, the short buildup times and high gain of the Q-switched Nd:YAG oscillator make single axial mode operation more difficult to achieve. A number of interferometric axial mode selection methods have been investigated including one or more tilted etalons [5], three-mirror resonators [6], resonant reflectors [7], and various figure “8” or ring resonator configurations [8]. These efforts resulted in single axial mode operation for only a fraction of the time and led to significant power reduction or resonator alignment instability.

The advantages of the unstable resonator [9] Nd:YAG source of high output energies with near diffraction limited spatial mode divergence have been clearly demonstrated [10], [11]. However, the spherically diverging wave propagating within the unstable resonator significantly reduces the spectral resolution of the interferometric axial mode selection elements [12] and increases the insertion loss of these elements. Two

intracavity tilted etalon elements, coupled with electronic Q-switch control, which allows prepulsing with microsecond instead of nanosecond buildup times [13], has led to single axial mode operation for 100 percent of the pulses from a stable resonator Q-switched Nd:YAG oscillator [14]. When the same technique was applied to an unstable resonator Nd:YAG oscillator, single axial mode operation at a significant reduction in output power and occasional two axial mode oscillation was achieved [15].

Failure of numerous attempts to achieve stable single axial mode operation from the unstable resonator Nd:YAG oscillator via a selective loss process eventually led us to the consideration of axial mode selection via the injection seeding process. Injection seeding was found to be easy to implement and extremely effective for obtaining long-term stable single axial mode operation of the unstable resonator Nd:YAG laser oscillator.

Injection locking has been widely applied to CW lasers for frequency locking and phase locking [16]. External signal injection also has been applied to pulsed dye lasers [17] and excimer lasers [18] to narrow the output bandwidth [19] and to improve the spatial mode quality [20]. However, in previous work, the oscillator output spectrum still consisted of many axial modes.

In this paper we show that injection seeding provides long term stable operation of the Q-switched Nd:YAG oscillator in single axial mode with Fourier transform limited spectral linewidth.

When an external signal is injected into a high gain laser oscillator whose axial mode separation is much wider than the bandwidth of the injected signal, an axial mode selection process takes place instead of the frequency locking process. We refer to this process as injection seeding. In the injection seeding process, laser oscillation occurs at the axial mode nearest the injected frequency and not at the frequency of the injected signal. Injection seeding for axial mode selection has been observed in CO<sub>2</sub> TEA laser oscillators [21], [22] and the Q-switched Nd:YAG laser oscillator [1].

In Section II we develop a model that describes axial mode selection by injection seeding of an external signal. The cavity field equations are developed which include the externally injected field. The cavity field equations and population rate equation for a nondegenerate two-level system are numerically solved in Section III.

Section IV describes the experimental studies of injection seeding using the unstable resonator Nd:YAG oscillator. A technique to obtain a long-term frequency stability is also described.

Manuscript received January 21, 1983; revised October 17, 1983. This work was supported by A.F.O.S.R. through Contract 80-0144. The work of G. Giuliani was supported by the N.A.T.O. Fellowship Program.

Y. K. Park was with the Department of Applied Physics, Edward L. Ginzton Laboratory of Physics, Stanford University, Stanford, CA 94305. He is now with the System and Research Center, Honeywell Inc., Minneapolis, MN.

G. Giuliani is with the Department of Physics, University of Rome, Rome, Italy. At the time of this work he was a visiting scholar at Stanford University, Stanford, CA 94305.

R. L. Byer is with the Department of Applied Physics, Edward L. Ginzton Laboratory of Physics, Stanford University, Stanford, CA 94305.

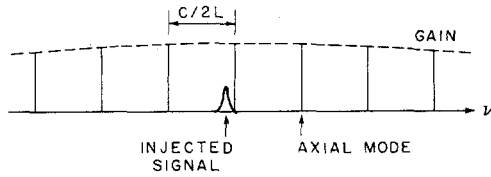


Fig. 1. An illustration of injection seeding for single axial mode selection.

## II. THEORETICAL MODEL

Fig. 1 illustrates the concept of the axial mode selection process by injection seeding of an external signal into a  $Q$ -switched or gain switched laser oscillator. An external signal at frequency  $\omega_i$  and with a bandwidth much narrower than the axial mode separation is injected near one of the axial mode frequencies  $\omega_c$  of the slave oscillator.

The injected field leads to the amplification of the axial mode field starting at the coupled injected field amplitude instead of from noise. If the bandwidth of the injected field is sufficiently narrow, the fields at the other resonator axial mode are not influenced by the injected field and start from noise. Single axial mode oscillation is accomplished if the mode, which is influenced by the externally injected field, reaches saturation and extracts energy from the gain medium earlier than the fields at the other noninjected axial mode resonances. A consequence of this model is that the output frequency occurs at the seeded axial mode frequency of the slave oscillator and not at input frequency of the master oscillator, as is the case for injection locking.

The laser system is governed by three basic equations in the semiclassical theory [23]: the cavity field equation, the polarization equation, and the population rate equations:

$$\ddot{\bar{E}}(t) + \frac{\dot{\bar{E}}(t)}{\tau_c} + \omega_c^2 \bar{E}(t) = -\frac{F}{\epsilon} \ddot{\bar{P}}(t) \quad (1)$$

$$\ddot{\bar{P}}(t) + \Delta\omega_a \dot{\bar{P}}(t) + \omega_a^2 \bar{P}(t) = -\frac{2\omega_a |\mu|^2 L}{3\hbar} \Delta N(t) \bar{E}(t) \quad (2)$$

$$\Delta \dot{N}(t) + \frac{\Delta N(t)}{T_1} = \frac{2}{\hbar\omega_a} \dot{\bar{P}}(t) \cdot \bar{E}(t). \quad (3)$$

Here  $\bar{E}(t)$  is the electric field,  $\bar{P}(t)$  is the macroscopic polarization of the gain medium,  $\tau_c$  is the cavity decay time,  $\omega_c$  is the cavity resonance frequency,  $\epsilon$  is the dielectric constant of the medium,  $F$  is the spatial mode filling factor,  $\omega_a$  and  $\Delta\omega_a$  are the atomic frequency and bandwidth,  $\hbar$  and  $\mu$  are Planck's constant and the dipole moment,  $\Delta N$  is the population difference,  $L$  is the Lorentz local field correction, and  $T_1$  is the relaxation time. The intensity is given by  $ce|\bar{E}(t)|^2/2$ .

We choose to describe the cavity fields by their Fourier relations

$$\bar{E}(t) = \frac{1}{2} [\bar{E}_\omega(t) e^{j\omega t} + \text{c.c.}]$$

$$\bar{P}(t) = \frac{1}{2} [\bar{P}_\omega(t) e^{j\omega t} + \text{c.c.}]$$

where  $\bar{E}_\omega(t)$  and  $\bar{P}_\omega(t)$  are complex time-varying phasor amplitudes at frequency  $\omega$ . If  $\bar{E}_\omega(t)$  or  $\bar{P}_\omega(t)$  have different

frequency components from the frequency of the injected field at time  $t$ , the frequency difference appears as a time derivative of the phase of  $\bar{E}_\omega(t)$  or  $\bar{P}_\omega(t)$ . It should be noted that the injected field remains at a constant frequency and that the cavity field suffers a phase shift during the amplification process.

Also, the above equations are strictly valid for near steady-state operation of a laser oscillator and may not be valid for the rapid buildup time reached in a high gain low- $Q$  oscillator. For the present model to be valid, the oscillator buildup process must extend over multiple roundtrips through the gain medium such that process can be approximated by a continuous evolution of the phase and amplitude of the field. Numerical calculations show that the model is a very good approximation for the  $Q$ -switched unstable resonator Nd:YAG oscillator which typically requires a 60 ns buildup time or 15 roundtrips to reach saturation following the opening of the  $Q$ -switch.

We are interested in the amplification of the cavity field  $\bar{E}_\omega(t)$  at the injected field frequency  $\omega_i$ .

Substituting the fields into (1), (2), and (3) and applying the slowly varying envelope approximation gives

$$\begin{aligned} \dot{\bar{E}}_{\omega_i}(t) + \left[ \frac{1}{2\tau} + j(\omega_i - \omega_c) \right] \\ \cdot \bar{E}_{\omega_i}(t) = -j \frac{\omega_i}{2\epsilon} F \bar{P}_{\omega_i}(t) \end{aligned} \quad (4)$$

and

$$\begin{aligned} \dot{\bar{P}}_{\omega_i}(t) + \left[ \frac{\Delta\omega_a}{2} + j(\omega_i - \omega_a) \right] \\ \cdot \bar{P}_{\omega_i}(t) = +j \frac{|\mu|^2 L}{3\hbar} \Delta N(t) \bar{E}_{\omega_i}(t) \end{aligned} \quad (5)$$

$$\begin{aligned} \Delta \dot{N}(t) + \frac{\Delta N(t)}{T_1} = \\ j \frac{1}{2\hbar} [\bar{P}_{\omega_i}(t) \cdot \bar{E}_{\omega_i}^*(t) - \bar{P}_{\omega_i}^*(t) \cdot \bar{E}_{\omega_i}(t)]. \end{aligned} \quad (6)$$

Here  $\bar{E}_{\omega_i}^*(t)$  and  $\bar{P}_{\omega_i}^*(t)$  are complex conjugates of  $\bar{E}_{\omega_i}(t)$  and  $\bar{P}_{\omega_i}(t)$ . For an atomic medium for which the polarization  $\bar{P}_{\omega_i}(t)$  responds linearly to the field  $\bar{E}_{\omega_i}$ , and for an injected frequency at the atomic frequency, (5) simplifies to

$$\bar{P}_{\omega_i}(t) = j \frac{2|\mu|^2 L}{3\hbar\Delta\omega_a} \Delta N(t) \bar{E}_{\omega_i}(t). \quad (7)$$

Equations (4) and (6) can be written by the use of (7) in the form

$$\dot{\bar{E}}_{\omega_i}(t) + \left[ \frac{1}{2\tau_c} - \frac{|\mu|^2 \omega_i L F}{3\epsilon\hbar\Delta\omega_a} \Delta N(t) + j\Delta\omega \right] \bar{E}_{\omega_i}(t) = 0 \quad (8)$$

and

$$\Delta \dot{N}(t) + \frac{\Delta N(t)}{T_1} = -\frac{2|\mu|^2 L}{3\hbar^2 \Delta\omega_a} \Delta N(t) |\bar{E}_{\omega_i}(t)|^2 \quad (9)$$

where  $\Delta\omega = \omega_i - \omega_c$  in (8) is the detuning parameter. Using the expression for the cross section at atomic resonance  $\sigma$ , given by

$$\sigma = \frac{2|\mu|^2 \omega_i L}{3\hbar ec \Delta\omega_a}, \quad (10)$$

(8) can be written in the simplified form

$$\dot{\bar{E}}_{\omega_i}(t) - m(t) \bar{E}_{\omega_i}(t) = 0 \quad (11)$$

where

$$m(t) = \frac{c\sigma F}{2} \Delta N(t) - \frac{1}{2\tau_c} - j\Delta\omega. \quad (12)$$

The cavity lifetime is defined by

$$\frac{1}{\tau_c(t)} = -\frac{1}{2\tau} \ln \{ R_1 R_2 T_Q^2(t) \} \quad (13)$$

where  $2\tau$  is one roundtrip time,  $R_1$  and  $R_2$  are the power reflectances of the front mirror and rear mirror, and  $T_Q(t)$  is the total internal power transmittance including the internal ohmic loss and the time-varying  $Q$ -switch loss. Using (13),  $m(t)$  can be rewritten as

$$m(t) = \frac{1}{2\tau} \left[ 2\gamma(t) l + \ln [\sqrt{R_1 R_2} T_Q] \right] - j\Delta\omega \quad (14)$$

where  $l$  is the length of the gain medium. It should be noted that (11) is the cavity field equation without the external field source.

In the presence of an injected field, (11) becomes

$$\dot{\bar{E}}_{\omega_i}(t) - m(t) \bar{E}_{\omega_i}(t) = f \{ m(t) \} \bar{E}_{\omega_i}^i(t). \quad (15)$$

where  $f \{ m(t) \}$  is the coupling coefficient determined by the boundary conditions. Here  $\bar{E}_{\omega_i}^i(t)$  is the phaser amplitude of the injected field defined by  $\bar{E}_{\omega_i}^i(t) = \frac{1}{2} [\bar{E}_{\omega_i}^i(t) e^{j\omega_i t} + \text{c.c.}]$ . It should be noted that this equation can be rewritten in a total differential equation form as

$$\frac{d}{dt} \bar{E}_{\omega_i}(t) e^{-\int m(t) dt} = f \{ m(t) \} \bar{E}_{\omega_i}^i(t) e^{-\int m(t) dt}. \quad (16)$$

The coupling coefficient  $f \{ m(t) \}$  is determined by imposing the Fabry-Perot boundary condition

$$E_{\omega_i} [2\tau(n+1)] = \bar{E}_{\omega_i}^i(2\tau n) + \bar{E}_{\omega_i}^i(2\tau n) e^{m(2\tau n)2\tau} \quad (17)$$

such that

$$f \{ m(t) \} = \frac{m(t)}{em(t)2\tau - 1}. \quad (18)$$

This expression for the coupling coefficient is valid in the paraxial approximation for an unstable resonator. In practice, geometrical factors associated with spatial mode overlap make an exact determination of  $f \{ m(t) \}$  difficult. Using (18), the cavity field equation (15) becomes

$$\dot{\bar{E}}_{\omega_i}(t) = m(t) \left[ \bar{E}_{\omega_i}(t) + \frac{1}{em(t)2\tau - 1} \bar{E}_{\omega_i}^i(t) \right] \quad (19)$$

Equation (19) describes the temporal behavior of the cavity field in the presence of the externally injected field. Equation (19) shows that the contribution of the injected field to the evolution of the cavity field is modulated by a time-varying Fabry-Perot envelope which is determined by both the parameters of the slave oscillator and the detuning parameter. During the initial buildup stage, the field is driven mainly by the second term which is the Fabry-Perot modulated injected field. However, when the gain is larger than the loss, the first term, which is the amplification term, soon dominates over the second term. The influence of the injected field on the cavity field then becomes insignificantly small. Therefore, the effect of the injected field is important only during the initial buildup time of the slave oscillator.

Equation (19) is identical with the cavity field equation that has been developed for CO<sub>2</sub> TEA lasers based on a Fabry-Perot model of the laser resonator. It reduces to give the equation that describes the CW injection locking solution in the steady-state limit [24].

Since the injected field  $E_{\omega_i}^i(t)$  can be either an externally injected field or an internally generated spontaneous noise field, (19) describes either the field at the seeded axial mode or the field at the nonseeded axial modes. For the injection seeded field, (19) can be separated into real and imaginary parts by writing the field amplitude and phase expressions as

$$\begin{aligned} \bar{E}_{\omega_i}(t) &= \mathfrak{E}(t) e^{j\phi(t)} \\ E_{\omega_i}^i(t) &= \mathfrak{E}^i(t); \quad \phi_i(t) = 0 \end{aligned}$$

where  $\mathfrak{E}(t)$  and  $\mathfrak{E}^i(t)$  are real amplitudes. Here the externally injected field  $\bar{E}_{\omega_i}^i(t)$  has zero phase and is detuned by  $\Delta\omega$  from the nearest cavity resonance mode. The real and imaginary parts of (19) describe the evolution of the amplitude and the phase, or the frequency shift which is the time derivative of the phase, of the injection seeded field. When the slave oscillator gain is turned on or when the  $Q$ -switch is opened, the initial conditions are assumed to be

$$\frac{d\mathfrak{E}}{dt} = \frac{d\phi}{dt} = 0.$$

At the nonseeded axial mode resonance, the field in the cavity field equation (19) is the internal spontaneous noise field. In addition, since  $\Delta\omega = 0$ , the imaginary part is identically zero. Based on an argument similar to that used by Lachambre *et al.* [21], the spontaneous noise power density for typical operating parameters of the unstable resonator Nd:YAG is  $10^{-5}$ - $10^{-6}$  W/cm<sup>2</sup> [25].

Equation (9), the population rate equation, applies when the injection seeded field is the only one which oscillates within the laser resonator. When other noninjected axial mode fields oscillate simultaneously, (9) must be modified to account for the total field present in the gain medium. If  $\phi(t)$  is the total photon density, (9) becomes

$$\Delta \dot{N}(t) + \frac{\Delta N(t)}{T_1} = -\sigma c \phi(t) \Delta N(t) \quad (20)$$

where  $\phi(t)$  is taken to be the incoherent sum of noise fields at each axial mode within the transition gain width including the

injection seeded field [21]. The initial condition,  $\Delta N(0)$ , is determined by measuring the single pass power gain  $G(0)$  where

$$G(0) = e^{\sigma \Delta N(0)l}.$$

To this point, the model is general and applies to all laser oscillators with a rapid increase in gain (gain switched lasers such as the CO<sub>2</sub> TEA lasers) or the rapid decrease of the cavity loss in the presence of high gain (*Q*-switched laser operation). The time-varying gain or *Q*-switch loss appears explicitly in the cavity field equations through the parameter  $m(t)$ .

In the next section the coupled equations for the field at the seeded axial mode, the fields at the nonseeded axial modes and the population density are solved numerically for the field amplitude and phase as a function of time. The numerical solutions use parameters of interest for *Q*-switched Nd:YAG oscillators. In particular, the values of  $T_Q(0)$  before the *Q*-switch opens and  $T_Q(\tau_Q)$  after the *Q*-switch opens were experimentally measured for the Nd:YAG unstable resonator oscillator which employed a KD\*P electrooptic *Q*-switch. The *Q*-switch transmittance is represented in the model by

$$T_Q(t) = T_Q(0) + [T_Q(\tau_Q) - T_Q(0)] \sin^2\left(\frac{\pi}{2} \frac{t}{\tau_Q}\right)$$

where  $\tau_Q$  is the opening time of the *Q*-switch and  $0 < t < \tau_Q$ .

The application of the model to Nd:YAG is further complicated by the spectral overlap of two transitions at 1.0642 and 1.0645  $\mu\text{m}$  [26], [27] and by the experimental observation that the transition is not homogeneously saturated on a time scale of *Q*-switched pulse lengths. The latter situation leads to a 15 percent decrease in the output energy from Nd:YAG for single axial mode operation relative to operation in two or more axial modes.

Although the model can be extended to include this effect [28], the basic equations are numerically solved for the simpler two-level homogeneously broadened situation.

### III. NUMERICAL SOLUTIONS OF THE CAVITY FIELD EQUATIONS

The model equations were solved by a numerical routine on a PDPLSI 11 minicomputer. Of particular interest was the evolution of the output frequency and the output power in time. Also of interest was the frequency detuning range over which injection seeding achieved single axial mode oscillation. The values required for the numerical computation are listed in Table I. These values were chosen to be consistent with the *Q*-switched unstable resonator Nd:YAG oscillator used in the experimental measurements.

As a specific example, consider a 10 MHz bandwidth seed pulse with 10 W/cm<sup>2</sup> intensity and 50 ns pulse width injected into an unstable resonator *Q*-switched Nd:YAG oscillator. The externally injected signal is assumed to be detuned 20 MHz from the nearest axial mode of the slave oscillator. The slave oscillator axial mode separation is 230 MHz and the slave oscillator is pumped twice above threshold at a single pass gain of 15.

Fig. 2 shows the numerical solution for the phase and amplitude of the field versus time. Fig. 2(a) is a plot of the time

TABLE I  
PARAMETERS FOR THE NUMERICAL COMPUTATION

$\Delta\nu_G = 1.5 \times 10^{11}$ Hz;	Nd:YAG FWHM gain bandwidth
$\sigma = 5 \times 10^{-19}$ cm <sup>2</sup> ;	stimulated emission cross section
$T_1 = 2.3 \times 10^{-4}$ s;	relaxation decay time
$G(O) =$ unsaturated	} 15 when pumped twice above threshold 4 when pumped 1.3 times above threshold
single pass gain	
$R_1 = 0.15$ ;	output coupler reflectance
$L = 65$ cm;	cavity length
$l = 5$ cm;	Nd:YAG rod length
$d = 0.63$ cm;	Nd:YAG rod diameter
$\tau_Q = 5 \times 10^{-8}$ s;	<i>Q</i> -switch opening time
$T_Q(O) = 0.07$ ;	high <i>Q</i> -switch loss transmittance
$T_Q(\tau_Q) = 0.6$ ;	low <i>Q</i> -switch loss transmittance

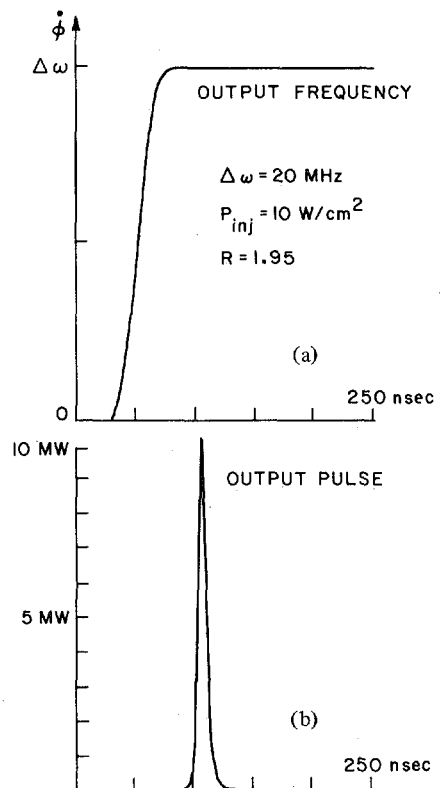


Fig. 2. A numerical solution of the transient injection seeding equations for (a) the phase of the field versus time, and (b) the amplitude of the field versus time.

derivative of phase  $\Phi$  versus time  $t$ . In this plot the  $y$ -axis corresponds to the instantaneous frequency of the injection seeded field. Fig. 2(a) shows that initially there is no frequency shift. Thus, the frequency of the injection seeded field is initially the same as the externally injected frequency as expected. However, as soon as the *Q*-switch opens, the frequency difference shifts from zero to  $\Delta\omega$ . This means that the injection seeded field frequency starts from the externally injected frequency at  $\omega_i$  but experiences a rapid phase change which causes the field frequency to shift toward the nearest axial mode of the slave oscillator at  $\omega_c = \omega_i + \Delta\omega$  during the amplification process. Fig. 2(b) shows that the output of a *Q*-switched pulse at the injection seeded field is produced when the frequency is completely shifted to the nearest slave oscillator axial mode. The noninjected axial mode amplitudes are not plotted in Fig.

2(b) because they are negligibly small compared to the seeded axial mode amplitude. The numerical results clearly show that the output pulse frequency is determined by the slave oscillator, not by the master oscillator. This behavior, which is contrary to the case of CW injection locking, was experimentally verified.

In CW injection locking the slave oscillator acts like a regenerative amplifier for the externally injected signal. If the frequency of the externally injected field is detuned from the resonance of the slave oscillator, the output initially follows the frequency of the externally injected field. At some detuning range the externally injected field no longer can force the slave oscillator gain below threshold for other slave oscillator axial modes and multi-axial mode oscillation occurs [16]. On the other hand, in injection seeding the steady-state regime is not reached. Instead, both the externally injected signal and the noise signals at the axial mode resonances of the slave oscillator grow simultaneously and compete to saturate the gain medium. Although the externally injected field is stronger than the noise field, it experiences a smaller gain because it suffers a phase change for each cavity traversal. The seeded axial mode field adds vectorially to the externally injected fixed phase field to produce a resultant field that changes in amplitude and in phase with time. This time-varying phase is equivalent to a frequency shift of the resultant field toward the nearest axial mode of the slave oscillator.

The detuning range for single axial mode operation is somewhat arbitrary because it is defined as the frequency detuning range over which the output power ratio between the seeded axial mode and the nonseeded adjacent axial mode always exceeds an arbitrarily set value. This is in contrast to CW injection locking where all axial modes of the slave oscillator remain below threshold except the injected mode. This difference makes the detuning range for single axial mode selection in the injection seeding much wider than the frequency locking range in the injection locking. Thus, experimentally, injection seeding leads to much easier met detuning ranges for single axial mode operation for *Q*-switched or gain switched lasers. The numerical result for the axial mode selection range is compared to the experimental result in the next section.

#### IV. EXPERIMENTAL RESULTS

##### A. Description of the Apparatus

Fig. 3 shows a schematic of the experimental setup used to investigate injection seeding. A TEM<sub>00</sub> mode stable resonator Nd:YAG oscillator with 35 cm cavity length served as the master oscillator. An air spaced 0.2 cm<sup>-1</sup> free spectral range etalon with finesse of 5 was used as the intracavity axial mode selective element. The master oscillator was pulsed at 10 Hz and operated at 5 J of flashlamp energy to minimize thermal effects on the 4 × 50 mm Nd:YAG rod. The quarter wave plates eliminated the spatial hole burning [29] of the Nd:YAG rod and the piezoelectric transducer controlled the cavity length. An electronically controlled *Q*-switching method [13], [14] was employed to provide single axial mode *Q*-switched pulses from the master oscillator. This method produces the *Q*-switched pulse following a microsecond buildup time prelude

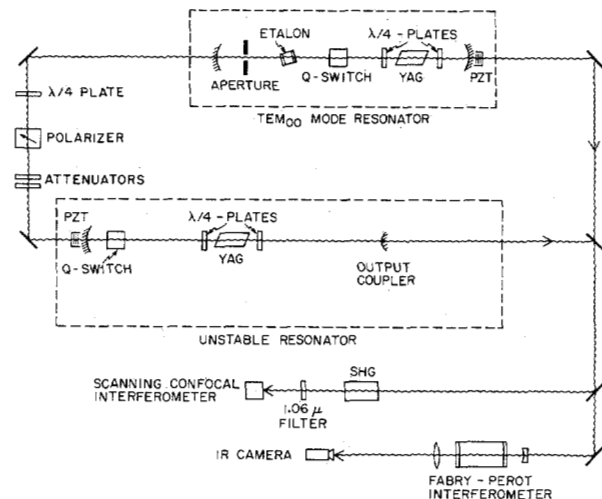


Fig. 3. A schematic of the experimental setup for single axial mode selection by injection seeding of the unstable resonator Nd:YAG oscillator.

spiking pulse. The spiking pulse thus experiences many passes through the intracavity etalon and, therefore, is effectively narrowed to a single axial mode.

The *Q*-switched Nd:YAG slave oscillator was of standard design with a 6.3 × 50 mm Nd:YAG rod within a 65 cm long confocal positive branch unstable resonator oscillator [10]. Again, two quarter wave plates were used to eliminate the spatial hole burning. It was not necessary to use line narrowing elements within the unstable resonator oscillator. A piezoelectric transducer controlled the cavity length to match one cavity axial mode frequency to the externally injected wave frequency. For both oscillators, the invar spaced cavity structure provided high mechanical stability and good compensation against thermal length expansion. The externally injected signal entered the slave oscillator through the 2 percent transmittance rear mirror and the injection power was controlled by attenuators. The two oscillators were effectively decoupled by a polarizer and quarter wave plate optical isolator and by the optical attenuators. No attempt was made to match the transverse modes of the injected wave and the slave oscillator. Thus, the oscillators were further decoupled by the poor spatial mode overlap.

The master oscillator was initially operated with an electrooptic *Q*-switch to generate high peak power pulses. This allowed a wide range of injection signal levels to be evaluated. It also allowed efficient harmonic generation so that the optical spectrum could be measured both at 1.06 and 0.532 μm. Measurements showed that, in agreement with the model, the un-*Q*-switched master oscillator provided more than adequate output power to injection seed the unstable resonator slave oscillator. For example, the 1 W peak power normal mode pulse from the master oscillator, after attenuation by absorption filters to less than 0.05 W and transmission by a 98 percent reflecting rear mirror of the unstable resonator oscillator, still provided more than adequate power at less than 1.0 mW peak power to injection seed the slave oscillator. This suggests the use of CW Nd:YAG or diode pumped Nd:YAG master oscillators for injection seeding.

The optical spectra of the two oscillators were monitored at  $1.06 \mu\text{m}$  with a 30 MHz resolution Fabry-Perot interferometer. A Tektronix 7904 oscilloscope with 500 MHz bandwidth was used to monitor the pulse shape. When the slave oscillator was operated with single axial mode output, the Fabry-Perot interferometer showed a clear change from a many axial mode to a single axial mode spectrum. The oscilloscope showed a change from the irregular pulse shape, which exhibited axial mode beating, to a smooth pulse shape which was completely free from any modulation at the cavity axial mode difference frequency. For high resolution measurements of the output optical spectra, a scanning confocal interferometer with 10 MHz resolution and 2 GHz free spectral range at  $0.53 \mu\text{m}$  was used. The  $Q$ -switched pulses were frequency doubled with a KD\*P crystal, monitored with the scanning interferometer, detected with a boxcar integrator, and recorded on a chart recorder. Scanning rates were held to longer than 2 min per free spectral range to fully time average the 10 Hz repetition rate spectrum from the laser oscillator.

### B. Optical Bandwidth

The 50 ns  $Q$ -switched pulses from the master oscillator had measured  $1.06 \mu\text{m}$  optical bandwidth of 10 MHz with  $\pm 5$  MHz frequency fluctuations. A major contribution to the frequency jitter was thermal fluctuations caused by a combination of flash-lamp energy variations and water cooling instabilities. The Fourier transform bandwidth of the 50 ns  $Q$ -switched pulses was calculated to be 9 MHz in good agreement with the measured value. When the single axial mode pulse from the master oscillator was injected to the unstable resonator and simultaneously the cavity axial mode was tuned to allow the injected wave frequency to be within the axial mode selection range, single axial output from the slave oscillator was obtained. Single axial mode operation was verified by both the Fabry-Perot interferometer spectrum and the pulse shape.

The  $Q$ -switched pulses from the slave oscillator and the output optical spectrum are shown in Fig. 4. The unstable resonator was pulsed at 10 Hz and operated at the 150 mJ per pulse output energy level with a 9 ns pulse width. Fig. 4(a) shows a multiple exposure of 200  $Q$ -switched pulses with better than 1 ns time resolution. The single axial mode operation is evident from the lack of axial mode beating modulation on the pulse. Single axial mode operation was also confirmed by the  $1.06 \mu\text{m}$  Fabry-Perot interferometer spectrum, which was observed using an IR vidicon camera. Fig. 4(a) also shows the very good pulse-to-pulse peak power stability. The Fourier transformed bandwidth of the  $Q$ -switched pulse is computed to be 50 MHz as shown in Fig. 4(b). Fig. 4(c) shows a scanned optical spectrum at  $0.53 \mu\text{m}$ . The bandwidth is measured to be 81.5 MHz at  $0.53 \mu\text{m}$  which corresponds to 57.8 MHz at  $1.06 \mu\text{m}$ . Considering that the scanned spectrum contains the output frequency jitter and is the convolution of the actual spectrum and the interferometer resolution, the measured bandwidth is in good agreement with the computed Fourier transform bandwidth. The clean shape of the optical spectrum recorded during a few minutes scan time also demonstrates that the slave oscillator produces frequency stable single axial mode  $Q$ -switched pulses.

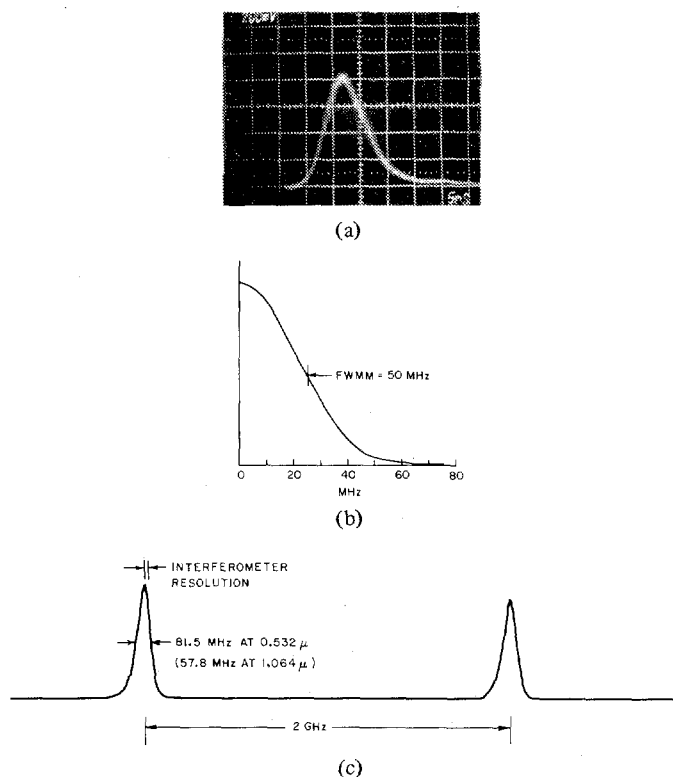


Fig. 4. (a) Multiple exposure of 200 pulses at 150 mJ output energy with a 1 ns temporal resolution at 5 ns/cm scale, (b) Fourier transform of the  $Q$ -switched pulse showing 50 MHz bandwidth, (c) optical spectrum of the injection seeded laser pulse at the second harmonic wavelength taken with the scanning confocal interferometer over a 2 min scan time. The two peaks are separated by the interferometer free spectral range of 2 GHz.

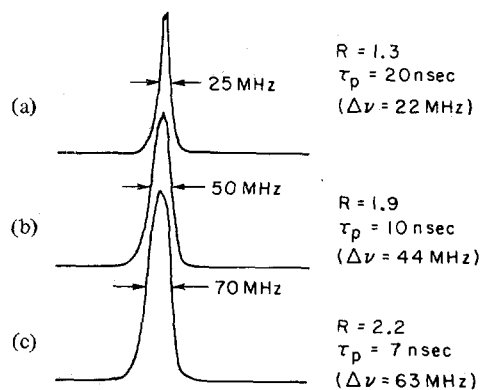


Fig. 5. Scanned optical spectra for various pulse widths of the output  $Q$ -switch from the slave oscillator. (a) For a 20 ns pulse width, (b) for a 10 ns pulse width, (c) for a 7 ns pulse width. The spectra were measured at  $0.53 \mu\text{m}$  wavelength and converted at  $1.06 \mu\text{m}$  with the factor of  $1/\sqrt{2}$  assuming Gaussian line shape.

Fig. 5 shows the scanned optical spectra for various  $Q$ -switched pulse widths. When the slave oscillator was operated 1.3 times above threshold, the pulse width was measured to be 20 ns. If the pulse shape is assumed to be Gaussian, the Fourier transform bandwidth is calculated to be 22 MHz, which is in good agreement with the measured bandwidth of 25 MHz, as shown in Fig. 5(a). At 1.9 times above threshold, Fig. 5(b) shows that the output bandwidth is 50 MHz, which agrees with 44 MHz Fourier transform bandwidth of 10 ns Gaussian pulse. At 2.2

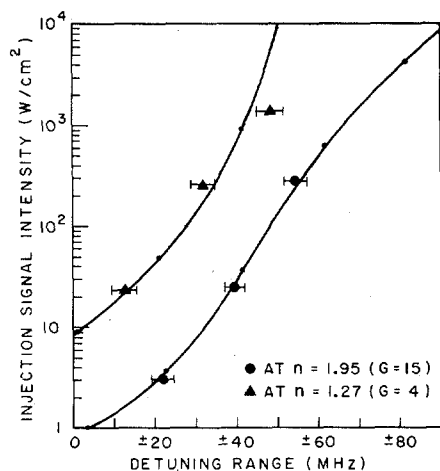


Fig. 6. A plot of the injection signal intensity versus axial mode selection range for two different gain levels of the slave oscillator. The axial mode spacing of the slave oscillator is 230 MHz and the bandwidth of the injected signal is 12 MHz. The injection signal intensity was measured before injecting into the rear mirror of the slave oscillator.

times above threshold the measured 70 MHz bandwidth in Fig. 5(c) agrees with the computed 63 MHz bandwidth of the 7 ns pulse.

### C. Output Frequency

An important prediction of the theory is that the output frequency of the slave oscillator is determined by the slave oscillator and not by the master oscillator. This was confirmed experimentally by tuning the cavity axial mode of the slave oscillator, but still within the axial mode selection range, and observing a wavelength change at  $1.06 \mu\text{m}$  using the Fabry-Perot interferometer and the infrared sensitive vidicon imaging system. On the other hand, if the frequency of the master oscillator was tuned within the axial mode selection range, no movement of the slave oscillator axial mode wavelength was observed. This result clearly demonstrates that the function of the injected signal in the Q-switched Nd:YAG oscillator is a selection of a particular axial mode by field enhancement.

### D. Axial Mode Selection Range

Fig. 6 shows that the axial mode selection range is increased for both high gain and high injection intensity. Fig. 6 also shows that the minimum required injection intensity for the single axial mode oscillation is extremely low for the Q-switched Nd:YAG oscillator. For a single pass gain of 15, which is a typical gain level for the unstable resonator Nd:YAG, the results show that only a few  $\text{W}/\text{cm}^2$  injection intensity are required to operate a single axial mode with a  $\pm 20$  MHz axial mode detuning range. This is an extremely low intensity, especially when compared to the injection intensity required to achieve CW injection locking.

### E. Buildup Time of the Output Pulse

The buildup time of the Q-switched pulse in the slave oscillator is expected to decrease with increased injection intensity because the Q-switch pulse builds up from the higher injection signal level. Fig. 7 shows the buildup for two different injection intensities. The upper trace of the photographs shows the

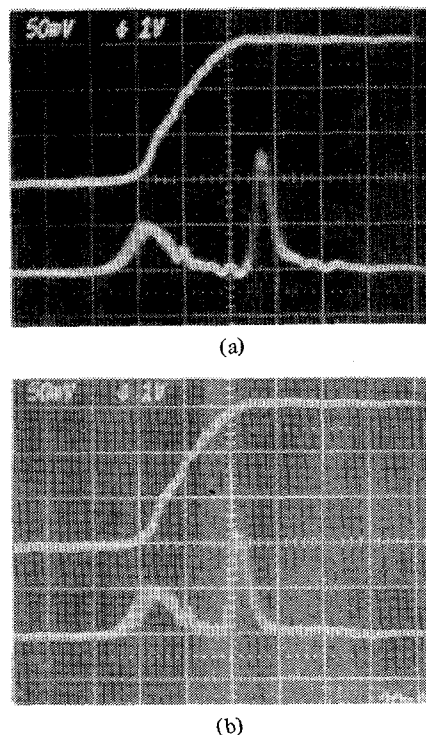


Fig. 7. Buildup time of the Q-switched pulse from the slave oscillator for two different injection intensity levels. (a) For  $I_{\text{inj}} = 1 \text{ W}/\text{cm}^2$ , (b) for  $I_{\text{inj}} = 1 \text{ kW}/\text{cm}^2$ . The upper trace is the Q-switch high voltage change with 1/1000 attenuation and inverted polarity. The lower trace shows an injected pulse and an output Q-switched pulse from the slave oscillator detected with the same detector.

Q-switched high voltage, and thus optical transmittance with the inverted polarity. The lower trace shows the output pulses of both the master oscillator and the slave oscillator monitored with the same detector. The output pulse of the slave oscillator was strongly attenuated to scale properly for display. Fig. 7(a) applies for  $1 \text{ W}/\text{cm}^2$  injection intensity and Fig. 7(b) for  $1 \text{ kW}/\text{cm}^2$  injection intensity. The buildup time is shorter for the high-intensity injected signal as expected.

### F. Long-Term Frequency Stabilization

Experimentally, we observed that injection seeding produces single axial mode operation of the unstable resonator Nd:YAG oscillator without any cavity length adjustments for periods of 2–5 min. This stability indicates the possibility of electronically providing feedback to lock the frequency of the injected field within the axial mode selection range, and thus to obtain long-term stable single axial mode operation. We considered and attempted a number of long-term stabilization methods. The use of a transfer interferometer reference cavity to which both master oscillator and slave oscillator were simultaneously locked, shown in Fig. 8, proved to be successful. The reference interferometer had a free spectral range of 3 GHz and finesse of 6, but was not thermally stabilized. The output frequency from both oscillators was locked to one side of the transmittance curve of the reference interferometer by two similar feedback control loops. Once set, we observed feedback controlled single mode operation for 10 min. before thermal drift of the interferometer exceeded the feedback loop control range. Our initial success with electronic stabilization of the

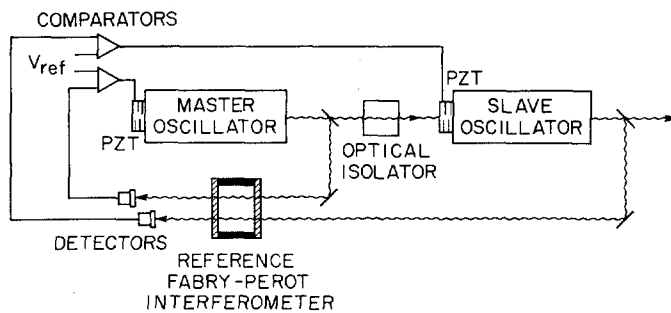


Fig. 8. A simplified schematic for long-term stabilization by electronic feedback control of the master and slave oscillator resonator frequencies.

master and slave oscillator using a transfer interferometer suggests that the output frequency of the single axial mode Nd:YAG can be absolutely stabilized by locking to a molecular or atomic absorption line such as molecular  $I_2$  at  $0.53 \mu\text{m}$  [30] or optogalvanic detected uranium in a hollow cathode discharge at  $1.06 \mu\text{m}$  [31], [32].

### V. CONCLUSION

Previously, intracavity interferometric loss selective techniques have been attempted as a means to obtain single axial mode operation of a  $Q$ -switched unstable resonator Nd:YAG laser oscillator. The results have been only partially successful due to the high gain and divergent wave front of the unstable resonator cavity. We have demonstrated that injection seeding is a very effective method for single axial mode selection in a high gain laser oscillator. In particular, stable Fourier transform limited bandwidth operation of a  $Q$ -switched unstable resonator Nd:YAG oscillator has been demonstrated.

We have developed a model to describe the axial mode selection process by injection seeding. The model predicts that the output frequency is that of the seeded axial mode frequency of the slave oscillator. The model is in agreement with the observed injection intensity and the detuning range for single axial mode selection. The model can be extended to other high gain laser oscillators and to transverse mode control by injection seeding.

The experiments carried out using an unstable resonator Nd:YAG oscillator have demonstrated that: 1) injection seeding provides very stable single axial mode  $Q$ -switched pulses with Fourier transform limited bandwidth without serious output power reduction; 2) that a very low power injection signal is adequate for single axial mode operation of the high gain Nd:YAG oscillator; 3) that the output frequency of the slave oscillator is not the externally injected signal frequency but is the slave oscillator axial mode frequency; and 4) that the axial mode selection range is much wider and more easily met than for steady-state injection locking.

The injection seeded single axial mode operation of the high peak power unstable resonator Nd:YAG source should greatly extend its usefulness for spectroscopy [33] and nonlinear interaction studies [15], [34] across the extended wavelength range now accessible by Nd:YAG pumped tunable sources.

### ACKNOWLEDGMENT

The authors wish to acknowledge helpful discussions with Prof. A. E. Siegman and T. Kane.

### REFERENCES

- [1] Y. K. Park, G. Giuliani, and R. L. Byer, "Stable single axial mode operation of an unstable resonator Nd:YAG oscillator by injection locking," *Opt. Lett.*, vol. 5, pp. 96-98, 1980.
- [2] H. G. Danielmeyer, "Stabilized efficient single frequency Nd:YAG lasers," *IEEE J. Quantum Electron.*, vol. QE-6, pp. 101-104, 1970.
- [3] W. Culshaw and J. Kannelaud, "Two component mode filters for optimum single frequency operation of Nd:YAG lasers," *IEEE J. Quantum Electron.*, vol. QE-7, pp. 381-387, 1971.
- [4] D. A. Draegert, "Efficient single longitudinal mode Nd:YAG laser," *IEEE J. Quantum Electron.*, vol. QE-8, pp. 235-239, 1972.
- [5] A. J. Egorov, V. V. Korobkin, and R. V. Scrov, "Single frequency  $Q$ -switched neodymium laser," *Sov. J. Quantum Electron.*, vol. 5, pp. 291-293, 1975.
- [6] R. N. Fleming, "The high energy broadly tunable coherent source," Ph.D. dissertation, M. L. Rep. 2521, 1976.
- [7] J. B. Shaw and G. A. Massey, "Temperature and wavelength dependent properties of multiplate reflectors," *IEEE J. Quantum Electron.*, vol. QE-13, pp. 950-954, 1977.
- [8] A triangular shape, a symmetric figure "8", and an asymmetric figure "8" shape ring resonator configuration along with the intracavity tilted etalon positioned at the arm of the collimated beam has provided partially successful single axial mode operation.
- [9] A. E. Siegman, "Unstable optical resonators for laser applications," *Proc. IEEE*, vol. 53, pp. 277-287, 1965; also —, "Unstable optical resonators," *Appl. Opt.*, vol. 13, pp. 353-367, 1974.
- [10] R. L. Herbst, H. Komine, and R. L. Byer, "A 200 mJ unstable resonator Nd:YAG oscillator," *Opt. Commun.*, vol. 21, pp. 5-7, 1977.
- [11] R. L. Byer and R. L. Herbst, "The unstable resonator YAG," *Laser Focus*, vol. 14, pp. 48-57, 1978.
- [12] Yu A. Anan'ev, N. S. Grishmanova, J. M. Petrova, and N. A. Sventsitskays, "Spectral selection of radiation emitted from lasers with unstable resonators," *Sov. J. Quantum Electron.*, vol. 5, pp. 408-410, 1975.
- [13] R. L. Herbst, Quanta Ray Inc., private communication. Double stepped  $Q$ -switching methods were also applied. See for example, D. C. Hanna, B. L. Davies, and R. C. Smith, "Single longitudinal mode selection of high power actively  $Q$ -switched laser," *Opt. Electron.*, vol. 4, pp. 249-256, 1972.
- [14] Y. K. Park and R. L. Byer, "Electronic linewidth narrowing method for single axial mode operation of  $Q$ -switched Nd:YAG lasers," *Opt. Commun.* vol. 37, pp. 411-416, 1981.
- [15] W. R. Trutna, Jr., Y. K. Park, and R. L. Byer, "The dependence of Raman gain on pump laser bandwidth," *IEEE J. Quantum Electron.*, vol. QE-15, pp. 648-655, 1979.
- [16] C. J. Buczek, R. J. Freiberg, and M. L. Skolnick, "Laser injection locking," *Proc. IEEE*, vol. 61, pp. 1411-1431, 1973.
- [17] J. J. Turner, E. I. Moses, and C. L. Tang, "Spectral narrowing and electro-optical tuning of a pulsed dye laser by injection locking to a cw dye laser," *Appl. Phys. Lett.*, vol. 27, pp. 441-443, 1975.
- [18] J. Goldhar, J. Dickie, L. P. Bradley, and L. D. Pleasance, "Injection locking of a xenon fluoride laser," *Appl. Phys. Lett.*, vol. 31, pp. 677-679, 1977.
- [19] T. Okada, M. Maeda, and Y. Miyazoe, "Spectral narrowing of a flashlamp pumped high energy dye laser by two stage injection locking," *IEEE J. Quantum Electron.*, vol. QE-15, pp. 616-623, 1979.
- [20] J. Goldhar, W. R. Rappart, and J. R. Murray, "An injection locked, unstable resonator rare gas halide discharge laser of narrow linewidth and high spatial quality," *IEEE J. Quantum Electron.*, vol. QE-16, pp. 235-241, 1980.
- [21] J. L. Lachambre, P. Laigne, G. Otis, and M. Noel, "Injection locking and mode selection in TEA  $CO_2$  laser oscillators," *IEEE J. Quantum Electron.*, vol. QE-12, pp. 756-764, 1976.
- [22] W. E. Schmid and S. D. Smith, "The injection locked single lon-

- gitudinal mode TEA CO<sub>2</sub> laser," Max Planck-Gesellschaft Int. Rep. D-8046, Garching, Germany, 1978.
- [23] R. H. Pantell and H. E. Puthoff, *Fundamentals of Quantum Electronics*, New York: Wiley, 1969.
- [24] Y. K. Park "Frequency and mode control of Q-switched Nd:YAG lasers," Ph.D. dissertation, Stanford Univ., Stanford, CA, 1980.
- [25] A. Yariv, *Quantum Electronics*, New York: Wiley, 1975.
- [26] W. Koechner, *Solid State Laser Engineering*, Berlin: Springer-Verlag, 1976.
- [27] H. G. Danielmeyer, "Single frequency lasers," in *Lasers*, vol. 4, A. K. Levine and A. J. DeMaria, Eds. Marcel Dekker, 1976, pp. 2-71.
- [28] Y. K. Park, "Frequency and mode control of Q-switched Nd:YAG lasers," Ph.D. dissertation, Stanford Univ., Stanford, CA, 1980, p. 24.
- [29] V. Evthuhov and A. E. Siegman, "A twisted mode technique in obtaining exactly uniform energy density in a laser cavity," *Appl. Opt.*, vol. 4, pp. 142-143, 1975.
- [30] R. L. Byer, R. L. Herbst, and R. N. Fleming, "A broadly tunable IR source," in *Laser Spectroscopy*, S. Haroche, J. C. Peby-Peyroula, T. W. Hansch, and S. E. Harris, Eds. Berlin: Springer-Verlag, pp. 207-225, 1975.
- [31] R. B. Green, R. A. Ketter, G. G. Luther, P. K. Schenck, and J. C. Travia, "Use of an opto-galvanic effect to frequency lock a continuous wave dye laser," *IEEE J. Quantum Electron.*, vol. QE-13, pp. 63-64, 1977.
- [32] D. S. King, P. K. Schenck, K. C. Smyth, and J. C. Travis, "Direct calibration of laser wavelength and bandwidth using optogalvanic effect in hollow cathode lamps," *Appl. Opt.*, vol. 16, pp. 2617-2619, 1977.
- [33] R. L. Byer and M. D. Duncan, "A 100 usec, reliable, 10 Hz pulsed supersonic molecular beam source," *J. Chem. Phys.*, vol. 74, pp. 2174-2179, 1981.
- [34] R. L. Byer, M. Duncan, E. Gustafson, P. Oesterlin, and F. Koenig, "Pulsed and cw molecular beam CARS spectroscopy," in *Laser*

*Spectroscopy V* (Springer Series in Optical Science), A. R. W. McKellar, T. Oka, and B. P. Stoicheff, Eds. Berlin: Springer-Verlag, pp. 233-241.

Y. K. Park, photograph and biography not available at the time of publication.

G. Giuliani, photograph and biography not available at the time of publication.



**Robert L. Byer** (SM'75) was born in Pasadena, CA, on May 9, 1942. He received the B.S. degree in physics from the University of California, Berkeley, in 1964, and the Ph.D. degree from Stanford University, Stanford, CA, in 1969.

After receiving the B.S. degree, he joined Spectra Physics, where he carried out research on ion lasers, single frequency helium neon lasers, and second-harmonic generation. He is currently Professor and Chairman of Applied

Physics at Stanford University. He is well known for his work in nonlinear optics, tunable laser sources, and applications of tunable sources to remote air pollution detection, optical pumping spectroscopy, and coherent anti-Stokes Raman spectroscopy. His recent research interests include nonlinear materials, tunable infrared generation by nonlinear crystal and Raman processes, and application of tunable sources to molecular spectroscopy, including high resolution CW CARS spectroscopy, optical pumping of new laser systems, and remote air pollution monitoring.

Professor Byer is a Fellow of the Optical Society of America and a member of the American Physical Society and the American Association for the Advancement of Science.